NEGATIVE PHASE AND LEADER SWITCHING IN NON-WEAKLY COUPLED TWO-CELL INHIBITORY NETWORKS *

VICTOR MATVEEV‡ and MYONGKEUN OH

Department of Mathematical Sciences, New Jersey Institute of Technology
University Heights, Newark, NJ 07102-1982, U.S.A.
‡*E-mail: matveev@njit.edu*

We examine the dynamics of a non-weakly coupled inhibitory network of two identical Morris-Lecar model neurons with type-I excitability, which was recently shown to exhibit stable alternating-order activity, whereby the spiking order of the two cells changes in each cycle of the oscillation. We provide an intuitive geometric description of such *leader switching* and demonstrate that the concept of negative phase allows to analyze the existence and stability of such alternating-order dynamics.

Keywords: non-weakly coupled oscillators, inhibitory network, leader switching, synchronization

1. Introduction

Understanding the dynamics and synchronization in inhibitory networks is a question of fundamental importance in neuroscience, since such networks play a crucial role in rhythmic activity in a variety of neural systems, from invertebrate central pattern generators (CPGs) to the mammalian brain.[2] Invertebrate CPGs in particular often contain simple two-cell inhibitory sub-networks that control different rhythmic motor behaviors. Therefore, characterizing the dynamics of such networks is relevant for a better understanding of the rhythmogenesis in biological inhibitory circuits. While recent work has revealed the synchronizing role of the inhibitory synaptic interaction,[2] it is known that non-weak coupling can destabilize phase-locked dynamics. In particular, Maran and Canavier[1] recently examined an inhibitory network of Wang-Buzsáki model neurons with type-I excitability,[3] and demonstrated that this network exhibits 2:2 mode-locked states

*Supported by the National Science Foundation grant DMS-0417416.

whereby the firing order of the coupled cells changes in each cycle of oscillation (see Fig. 1). We find that such behavior (termed "leap-frog" spiking or "leader switching"[4]) is a more general property of a subclass of non-weakly coupled type-I oscillators characterized by slow dynamics of membrane potential upon hyperpolarization, and in particular can be achieved in a network of simpler Morris-Lecar (ML) model neurons. We present an intuitive geometric description of leader switching by examining the phase space trajectory of the two cells, and establish the most fundamental conditions for the existence and stability of such dynamic behavior.

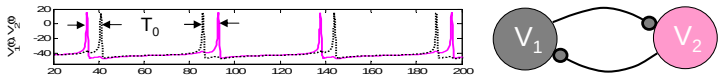

Fig. 1. Time-course of membrane potentials of the two non-weakly coupled ML cells, $V_1(t)$ and $V_2(t)$, showing periodic leader switching ("leap-frog" spiking). Note that the interval between two spikes of the same cell equals the intrinsic (unperturbed) oscillation period, T_0.

2. Phase-plane geometry of alternating-order spiking.

Figure 2A shows the phase-space geometry of the ML model neuron (equations and parameters given in Appendix). This model has two dynamical degrees of freedom: the membrane potential, V, and the activation of the outward K^+ current, w. The V-nullcline is cubic-shaped, while the w-nullcline is sigmoidal. In the absence of synaptic coupling, the V-nullcline is in its upper position; the two nullclines intersect at an unstable fixed point, and there exists a stable limit cycle shown in blue, which represents an electric pulse (an *action potential*; see V time-course in Fig. 1). This limit cycle results from the push-pull interaction between the voltage-activated inward Na^+ current and the more slowly activating outward K^+ current (first two terms in the Kirchhoff current balance, Eq. A.1).

The two identical ML cells are coupled by inhibition, which means that a V spike in one cell (the *presynaptic* cell) will introduce a hyperpolarizing current into its partner cell (the *postsynaptic* cell). This has the effect of lowering the V nullcline of the postsynaptic cell (gray curve in Fig. 2A), which in its lowered position intersects the w nullcline at a *stable* fixed point, where the postsynaptic cell will be transiently trapped. This transient suppression (lasting for the duration of the synaptic current) allows the

presynaptic cell to advance past the postsynaptic cell along its trajectory, as described by the sequence of panels in Fig. 2B.

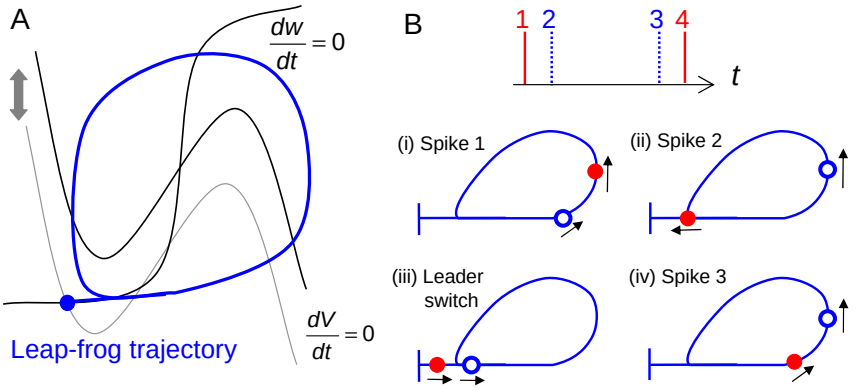

Fig. 2. Phase plane dynamics of each ML cell during alternating-order spiking. (A) Nullclines of the ML model. Synaptic inhibition lowers the V-nullcline of a cell, transiently trapping it at a stable fixed point. Tadpole-shaped blue curve indicates the trajectory of each cell during one cycle of the alternating-order spiking shown in Fig. 1. Note that it overlaps the w-nullcline during the hyperpolarized phase of the oscillation. (B) The sequence of four panels describes the leap-frog spike sequence at the top, with filled red and open blue circles representing the two cells: (i) "red" cell spikes; (ii) "blue" cell spikes, pushing the "red" cell into the subthreshold branch of the trajectory (tadpole tail); (iii) "blue" cell bypasses the "red" cell along the unperturbed limit cycle; (iv) "blue" cell spikes again. The process then repeats itself, with the "red" cell spiking next.

Interestingly, the mechanism just described is valid even in the limit of infinitely short synaptic interaction, whereby the synaptic current introduces an instantaneous hyperpolarization into the postsynaptic cell. This is a surprising fact, since such an instantaneous input produces a shift in the potential, but does not lower the V-nullcline, and therefore does not create a meta-stable fixed point where the cell could be transiently trapped. To understand the existence of leap-frog spiking in this *pulse-coupled* case, we examined the *isochrons* of the model, shown in Fig. 3. An isochron is a powerful concept allowing to analyze the response of oscillators to perturbations;[5–7] it represents a set of points that asymptotically approach the same point on the limit cycle. An isochron foliation therefore completely describes the long-term behavior of the system starting at any initial position in the basin of attraction of the limit cycle, in terms of the point on

the cycle that this trajectory will eventually approach. Now, if the presynaptic cell spikes while the postsynaptic cell is on the bottom part of the trajectory (where it in fact spends most of the time), inhibition produces a left-ward shift (negative V pulse) onto an isochron that curls around the limit cycle, intersecting it at a position (filled circle) that is retrograde to the position of the presynaptic cell at spike-time (open circle). This means that the inhibition retards the dynamics of the postsynaptic cell sufficiently to allow the presynaptic cell to advance ahead of it, reversing the spiking order of the two cells. Such strong retardation is a result of slow dynamics of V along the portion of the limit cycle overlapping the w-nullcline, which constitutes the slow manifold of the system, due to fast closing of K^+ channels (fast w dynamics) at hyperpolarized potentials.

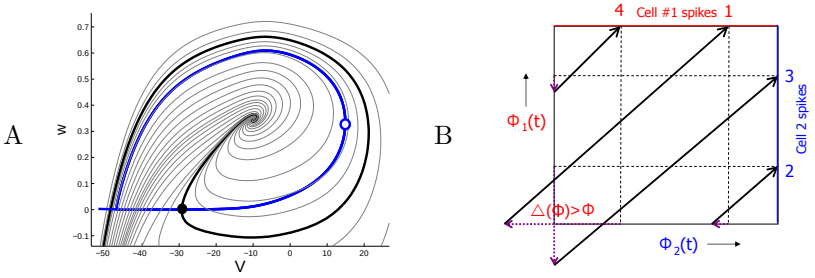

Fig. 3. Leap-frog spiking in a pulse-coupled network. (A) Isochron foliation of the model ML cell. Note the characteristic curling of the isochrons around the limit cycle. (B) Phase-reduced description of the alternating-order spike sequence in top panel of Fig. 2B. Top and right boundaries correspond to spikes of cell 1 (red) and cell 2 (blue), respectively. The trajectory is discontinuous across these boundaries, due to synaptic inhibition received at each boundary crossing (arrows).

If the oscillators stay close to their limit cycles, isochrons allow to reduce the n-dimensional state space to a one-dimensional *phase* variable defining position along the limit cycle, since there is a (surjective) mapping from any state-space position onto the corresponding isochron. This 1-D phase variable can be simply defined as the time variable of the limit cycle trajectory, normalized by the unperturbed oscillation period. Such dimensional reduction is in fact the key to analyzing weakly-coupled oscillator dynamics,[5,7] but we also find it useful in our case of non-weak coupling. In Figure 3B, we qualitatively describe leader switching as a trajectory on the surface of a 2-D phase torus formed by the 1-D phase variables of each cell. The top boundary of the torus corresponds to the spike of cell 1, which sends

an inhibitory pulse to cell 2, pushing the trajectory leftward as it is resets (wraps around) in the vertical direction. Analogously, the right boundary corresponds to the spike of cell 2, which sends an inhibitory pulse to cell 1, producing a downward trajectory shift. Note that leader switch only occurs if these synaptic deflections (phase resets, $\Delta(\phi)$) are strong enough to push the trajectory outside of the phase domain, into the region corresponding to *negative* phase values. Such strong phase resets correspond to the isochrons intersecting the limit cycle at a position retrograde to the peak of an action potential, as described above (panel A). Finally, note that in the absence of coupling the trajectory is a straight line of slope 1, given the simple definition of phase as normalized time.

3. Existence and stability of periodic leader switching

Figure 4A "unwraps" the phase-torus in Fig. 3B, plotting the phase time-course for one of the two cells. Phase is reduced (delayed) by amounts Δ in response to each spike of the partner cell. The dependence of phase delay on cell's current phase, $\Delta(\phi)$, is shown in Fig. 4B; it is known as the *the spike-time response curve* (STRC). It is computed numerically by measuring the lengthening of the cell's period produced by synaptic inputs applied at different times (phases) since the peak of the cell's action potential, which is defined as the zero phase point. The STRC is a powerful tool in analyzing both weakly and non-weakly coupled oscillator dynamics.[4–8] Following Ref. 1, we will now use the STRC to analyze the existence and stability of leap-frog spiking, but will restrict ourselves to the case of a homogeneous network for simplicity. Our derivation is a direct extension of Ref. 8 to the case of negative phase values, previously viewed as problematic.

Alternating-order firing is completely characterized by the inter-spike phase sequence labeled $\{\phi_1, \phi_2\}$ in Fig. 4A; we will construct the return map relating these phase intervals. Note that ϕ_1 is the phase of cell 1 (*red* spike and *red* trace) at the arrival time of the first synaptic pulse from the pre-synaptic cell (dashed blue line), where phase is defined as time since preceding spike, normalized by unperturbed oscillation period. The amount of phase delay induced by this input equals $\Delta(\phi_1)$. For sufficiently strong synaptic inhibition this phase reset satisfies $\Delta(\phi_1) > \phi_1$ which delays the first passage time to next spike of cell 1 to a value greater than 1, the intrinsic oscillation period. As a result, cell 2 has a chance to spike again (second dashed line), after a phase interval corresponding to the unperturbed oscillation period, $\Delta\phi = 1$, since cell 2 receives no input from cell 1 during this period. This second synaptic current arrives when the phase of cell 1

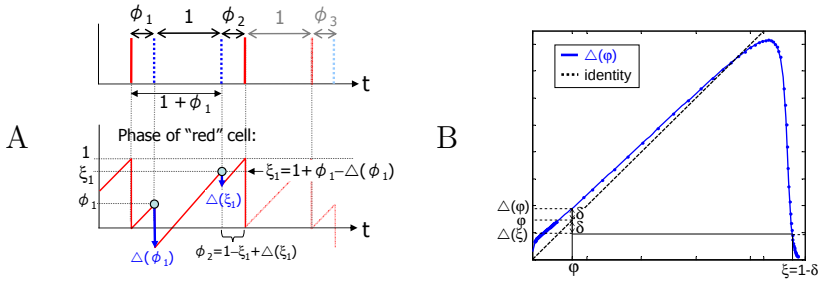

Fig. 4. Phase-map analysis of alternating-order spiking. (A) Spike sequence (top) and the phase time-course of one of the two cells (bottom) during leap-frog spiking. During one oscillation cycle, each cell spikes twice between two spikes of the partner cell. Phase intervals ϕ_i are inter-spike intervals normalized by the unperturbed period of each oscillator. The phase difference between two dashed spikes equals 1 (the unperturbed period). Phase delays due to each of the two spikes (blue arrows) equal $\Delta(\phi_1)$ and $\Delta(\xi_1)$, where ξ_1 is the phase of the cell at the time of arrival of the second input, $\xi_1 = 1 + \phi_1 - \Delta(\phi_1)$. The second inter-spike interval ϕ_2 is found by the first-passage time condition $\xi_1 - \Delta(\xi_1) + \phi_2 = 1$. (B) STRC of each ML cell, $\Delta(\phi)$, for $\bar{g}_{syn} = 0.2$. Equilibrium inter-spike phase difference ($\phi = 0.144$) in the alternating-order state satisfies Eq. 3. Note that $\delta = \Delta(\phi) - \phi = \phi - \Delta(\xi)$, where ξ is the phase of the postsynaptic cell at the time of arrival of the second spike, $\xi = 1 - \delta$. Here $\delta = 0.0468$, and $\Delta(1 - \delta) = 0.095$.

equals $\xi_1 \equiv 1 + \phi_1 - \Delta(\phi_1)$, taking into account the delay due to the first spike; therefore, it induces a phase delay equal to $\Delta(1 + \phi_1 - \Delta(\phi_1))$. It is only after receiving this second input that cell 1 finally has a chance to spike, after a phase interval defined as ϕ_2. The total phase delay due to both inputs is thus equal to $\phi_1 + \phi_2 = \Delta(\phi_1) + \Delta(1 + \phi_1 - \Delta(\phi_1))$. Therefore, the return map for the phase intervals ϕ_i is given by

$$\phi_2 \equiv \Phi(\phi_1) = \Delta(\phi_1) + \Delta(1 + \phi_1 - \Delta(\phi_1)) - \phi_1 \tag{1}$$

or, expressed in terms of the phase of the post-synaptic cell at the time of arrival of the second spike, $\xi_1 = 1 + \phi_1 - \Delta(\phi_1)$:

$$\phi_2 \equiv \Phi(\phi_1) = 1 + \Delta(\xi_1) - \xi_1 \tag{2}$$

Fixed points of this map correspond to the periodic leap-frog activity:

$$\phi = 1 + \Delta(\xi) - \xi \tag{3}$$

Since $\xi \equiv 1 + \phi - \Delta(\phi)$, this condition can be written in a more symmetric form

$$\phi = \frac{\Delta(\phi) + \Delta(\xi)}{2} \tag{4}$$

Taking into account the domain constraints $\xi \leq 1$, $\phi \leq 1$, we also have

$$\Delta(\phi) > \phi, \ \Delta(\xi) < \xi \tag{5}$$

Conditions **??** are examined geometrically in Fig. 4B. Note that the synchronous firing solution $\{\phi = 0^+, \xi = 1^-\}$ always satisfies the periodicity condition (4), if one assumes $\Delta(0^+) = \Delta(1^-) = 0$. If the inequality $\xi \leq 1$ is violated (i.e. when $\Delta(\phi) < \phi$), the cells fire sequentially, so their firing order does not alternate, while the violation of the condition $\Phi(\phi) \leq 1$ (i.e. if $\Delta(\xi) > \xi$) indicates that the postsynaptic cell will emit more than two consecutive spikes.

Stability of the periodic leap-frog spiking depends on the value of the derivative of the phase map given by Eq. 4 at equilibrium:

$$\Phi'(\phi) = [\Delta'(\xi) - 1][1 - \Delta'(\phi)] \tag{6}$$

The fixed point will be stable if $|\Phi'(\phi)| < 1$; an equivalent stability condition was derived in Ref. 1. The stability of synchronous firing is determined by an analogous map slope expression, with $\phi = 0^+$ and $\xi = 1^-$ (Eq. 12 in Ref. 8). Since $\Delta'(1^-) \approx 0$ in the ML model (see Fig. 4B), the bifurcation from synchronous to leap-frog firing occurs when the slope $\Delta(0^+)$ becomes greater than 2, forcing ϕ to increase (and ξ to decrease) until the stability condition is satisfied. Thus, the characteristic sharp initial rise of $\Delta(\phi)$ followed by a less steep increase at larger ϕ evident in Fig. 4B is essential for the transition from synchronous to leap-frog spiking. This feature corresponds to the characteristic dip to negative values in the phase transition return map noted in Ref. 1.

4. Effect of variation in coupling strength

Maran and Canavier[1] found that increasing the coupling strength causes the network to undergo a period-doubling cascade to chaos, whereby the synchronous dynamics seen for weak coupling transitions to leap-frog spiking in Fig. 1, followed by higher-period alternating-order states. Note that this period-doubling is readily explained by the map, Eq. , if one assumes a simple scaling between the coupling strength and the maximal amplitude of the STRC. In order to confirm this, we replaced the STRC with a simple quadratic function satisfying the leap-frog existence conditions established above, and "emulated" (artificially generated) the corresponding spike event sequence for different values of the amplitude of the quadratic STRC. The resulting bifurcation diagram was in good qualitative agreement with the bifurcation structure of the full ML network.

5. Concluding remarks: leap-frog spiking in 1-D models

Finally, we note that the above analysis can be used to show stable leap-frog spiking in even simpler 1-D models, for example in networks of quadratic integrate-and-fire neurons with a finite reset, and in networks of 1-D phase oscillators with continuous synaptic interaction.

Acknowledgments

This work was partially supported by the NSF grant DMS-0417416.

Appendix A. Morris-Lecar model parameters

We consider two identical Morris-Lecar neurons[11] with type-I excitability:[12]

$$C\frac{dV}{dt} = -\bar{g}_{Ca}m_\infty(V)(V-V_{Ca}) - \bar{g}_K w(V-V_K) - \bar{g}_L(V-V_L) - I_{app} - I_{syn}$$
$$\frac{dw}{dt} = \frac{w_\infty(V)-w}{\tau_\infty(V)} \tag{A.1}$$

$m_\infty(V) = [1+\tanh((V+12)/18)]/2$, $w_\infty(V) = [1+\tanh((V+8)/6)]/2$, $\tau_\infty(V) = 3/[2\cosh((V+8)/12)]$, $C = 2\mu\text{F/cm}^2$, $I_{app} = -14\mu\text{A/cm}^2$, $V_{Ca} = 120\text{mV}$, $V_K = -84\text{mV}$, $V_L = -60\text{mV}$, $g_{Ca} = 4\text{mS/cm}^2$, $g_K = 8\text{mS/cm}^2$, $g_L = 2\text{mS/cm}^2$. Unperturbed limit cycle period is 45ms.

Cells are synaptically coupled by $I_{syn} = \bar{g}_{syn}s(t)(V-V_{inh})$ where $\bar{g}_{syn}$ is the peak synaptic conductance and $V_{inh} = -80\text{mV}$. Each synaptic gating variable $s_i(t)$ (i=1,2) is controlled by the presynaptic cell potential, $V_{j\neq i}$:

$$\frac{ds_i}{dt} = -\frac{s_i}{\tau_{syn}}\sigma(V_{th}-V_j) + \frac{1-s_i}{\tau_\gamma}\sigma(V_j-V_{th}) \tag{A.2}$$

where $V_{th} = -3$ mV is the synaptic threshold, $\sigma(x) = [1+\tanh(4x)]/2$, and $\tau_{syn} = 1$ ms and $\tau_\gamma = 0.2$ ms are the synaptic decay and rising time constants, respectively.

References

1. S. K. Maran SK and C. C. Canavier, *J. of Comput. Nerosci.* **24**, 037(2008).
2. J. A. White *et al.*, *J. of Comput. Neurosci.* **5**, 005 (1998).
3. X.-J. Wang and G. Buzsáki, *J. Neurosci.* **16**, 6402 (1996)
4. C. D. Acker, N. Kopell and J. A. White, *J. Comput. Neurosci.* **15**, 71 (2007).
5. A. T. Winfree, *The Geometry of Biological Time,* Springer (2001).
6. Y. Kuramoto, *Chemical Oscillations, Waves, and Turbulence,* Springer (1984).
7. E. M. Izhikevich and Y. Kuramoto, *Encycl. Math. Phys.* **5**, 448 (2006).

8. P. Goel and G. B. Ermentrout, *Physica D.* **163**, 191 (2002).
9. Ermentrout GB (1996). Neural Computation 8:979-1001.
10. E. Marder and R. L. Calabrese, *Physiol. Rev.* **76**, 687 (1996).
11. C. Morris and H. Lecar, *Biophys. J.* **35**, 193 (1981).
12. J. Rinzel and B. Ermentrout, *Methods in Neuronal Modeling, Eds. C. Koch and I. Segev*, MIT Press (1998).